Nobiletin Down-regulates SKP2-p21/p27-CDK2 Axis to Inhibit Tumor Progression and Shows Synergistic Effect with Palbociclib on Renal Cell Carcinoma

Tingting Chen
Xinqiao Hospital
Liu Liu
Huazhong University of Science and Technology
Xiaoyan Hu
Xinqiao Hospital
Kai Wang
Nanchang University Second Affiliated Hospital
Tao Zhou
Xinqiao Hospital
Xi Luo
Southwest Hospital
Longkun Li
Xinqiao Hospital
Weihua Fu
Xinqiao Hospital
Jie Xu (xujie1981@tmmu.edu.cn)
Xinqiao Hospital https://orcid.org/0000-0001-6700-7096

Research

Keywords: Nobiletin, SKP2, Palbociclib, Synergistic, Renal Carcinoma

Posted Date: April 10th, 2020

DOI: https://doi.org/10.21203/rs.3.rs-19110/v1

Abstract

Background: Natural extracts can enhance the efficacy and sensitivity of chemotherapeutic drugs, including nobiletin. However, the possible role and underlying mechanisms of nobiletin in cancer including Renal cell carcinoma (RCC) are still unclear.

Methods: Cell proliferation, cell cycle and apoptosis analysis, colony-forming assays, immunoblotting analysis and qRT-PCR analysis were performed to investigate how nobiletin inhibits RCC cell proliferation in vitro. Nude mouse model was used to measure in vivo efficacy of nobiletin and its combination with palbociclib.

Results: Nobiletin induced G1 phase cell cycle arrest, apoptosis, and proliferative inhibition in RCC Cells. Mechanistically, nobiletin inhibited activation of oncogene SKP2, leading to the accumulation of tumor suppressors and apoptosis-inducing substrates such as p21 and p27 to inhibit cell proliferation, eventually inhibit tumor formation. Intriguingly, we further found that sensitivity of palbociclib was associated with SKP2 protein level. Furthermore, in vitro and vivo results, dual inhibition of nobiletin and palbociclib showed synergistic lethality.

Conclusion: Combination nobiletin and palbociclib may serve as a potential therapeutic strategy for renal cancer.

Background

Renal cell carcinoma (RCC) is the sixth most common cancer in men and the 10th in women, accounting for 5% and 3% of all new cancer cases, respectively[1]. Despite higher proportion of indolent and localized tumors identified partly due to widespread use of abdominal imaging techniques, there are still up to 17% of patients present with distant metastases at the time of diagnosis[2]. In addition, approximately one quarter patients with localized RCC develops distant metastasis after radical surgery. Once progression to metastatic RCC (mRCC), the treatment is still an intractable problem, despite the introduction of novel agents targeting different pathways including angiogenesis, mTOR inhibitors, immune checkpoint inhibitors. Comparing with cytokine treatment (interferon alpha or interleukin-2), targeted therapies have really significantly improved the clinical outcomes of mRCC[3]. Sunitinib as first-line therapy form RCC achieved significantly longer progression-free survival (PFS) (11 versus 5 months), overall survival (OS) (26.4 versus 21.8 months) and a better response rate (31% versus 6%) than interferon alpha group[4, 5]. However, RCC is the highly heterogeneous tumor. Ascribe to the intratumor and intertumor heterogeneity, the objective response rates of current first-line agents form RCC were about 30% and even lower[3, 6]. Even more disastrous is resistance to drugs eventually develop in nearly all patients, which have driven sustained efforts to identify novel targets and treatment strategies for mRCC, in order to achieve the better clinical outcomes.

Many natural extracts are the potential antitumor drugs because of its low toxicity and few side effects[7, 8]. Some extracts have anti-tumor pharmacological effects and can be used as a regulator of multi-drug

resistance to increase the sensitivity of cancer cells to chemotherapy[9]. Nobiletin is a typical example, which is an O-methylated flavonoid found mainly in citrus peel. Previous studies have shown that nobiletin can significantly inhibit growth and metastasis of several cancer cell both in vitro and in vivo through multiple pathways [10, 11]. Of note, nobiletin can extremely inhibit cell proliferation through attenuating the expression of cyclin D1, CKD2, CKD4 and E2F[12]. So far, few studies have reported the effects of nobiletin in kidney cancer. Limited data showed that nobiletin could inhibit cells viability and hypoxia-induced migration of RCC cell lines, and the SRC/AKT, NF-κB and Wnt/β-Catenin signaling pathways might involve in the effects[13, 14]. A study reported that nobiletin induced G0/G1 cell cycle arrest in RCC cells, but did not explain mechanism of action of nobiletin in cell cycle arrest[14]. Therefore, the possible role and underlying mechanisms of nobiletin in cancer including RCC are still unclear.

Cell-cycle dysregulation is prevalent in multiple malignancies, including RCC[15]. G1-S cell cycle transition is mainly regulated by two cyclin/CDK complexes, cyclin D-CDK4/6 and cyclin E-CDK2. Cyclin/CDK complexes phosphorylates the G1 gatekeeper Rb, causing the release of S-phase–specific transcription factors, such as E2F. E2F causes the transcriptional induction of Cyclin E, which in turn partners with CDK2 to further phosphorylate RB and irreversibly cause the transition into S phase[16]. Therefore, the exploration of targeted anti-tumor drugs capable of blocking the progression of tumor cells from G0/G1 phase to S phase has become one of the hot spots in the development of anti-tumor drugs. Palbociclib is an orally active, potent, and selective inhibitor of CDK4 and CDK6, which blocks RB phosphorylation at low drug concentrations[17]. In addition, many solid tumors are often directly inherited, epigenetic or transcriptional modification leads to loss of control of the CCND-CDK4/6-INK4-Rb signaling pathway[18–22]. Because of the central role in tumor genesis and progression, CDK4/6 might represent a valid therapeutic target for cancer treatment in a broad spectrum of solid tumors. Several phase II studies tested palbociclib monotherapy in a broad variety of solid tumors, namely well-differentiated or dedifferentiated liposarcoma (WD/DDLS)[23, 24], HR + and triple negative breast cancer (TNBC)[25]. Moreover, a study has shown that palbociclib could inhibit of proliferation in RCC at nanomolar concentrations[26]. However, sustained G1-S phase cyclin expression and other early and late adaptations mediated by bypass signal transduction limit the effectiveness of CDK4/6 inhibitors[27]. For instance, some papers showed that palbociclib blocked cells in the G1 phase by inhibiting CDK4/6 activity, but it did not inhibit CDK2 activity, and the inhibition effect of RB phosphorylation could be reversible by CDK2 to produce drug resistance[28]. One candidate that could compensate for loss of CDK4/6 activity is CDK2, so a therapy that simultaneously inhibits both kinases at the outset might offer therapeutic advantages of palbociclib.

In this study, we observed that nobiletin did induce G1-phase cell cycle arrest, apoptosis, and proliferative inhibition in RCC Cells. Mechanistically, nobiletin inhibited activation of oncogene SKP2, leading to the accumulation of tumor suppressors and apoptosis-inducing substrates such as p21 and p27 to inhibit cell proliferation, eventually inhibit tumor formation. Intriguingly, we further found that sensitivity of palbociclib was associated with SKP2 protein level. Furthermore, in vitro and vivo results, dual inhibition of nobiletin and palbociclib showed synergistic lethality, suggesting that nobiletin could reverse drug

resistance of palbociclib. Therefore, this combined regimen may serve as a potential therapeutic strategy for renal cancer.

Material And Methods

Reagents and cell cultures

Nobiletin (#HY-N0155), palbociclib (#HY-50767), MG-132(#HY-13259) and Cycloheximide (#HY-12320) were purchased from Selleck Chemicals, and dissolved in dimethyl sulfoxide (DMSO) (Amresco, #N182) and stored at -20 °C. The RCC lines (786-O, 769-P, OSRC-2 and Caki-1) and immortalization of epithelial renal cell line (HK-2) were purchased from the Zhong Qiao Xin Zhou Biotechnology Co., Ltd. (Shanghai, China). 786-O, 769-P, and OSRC-2 cell lines were routinely maintained in RPMI-1640 medium. Caki-1 cell lines was grown in McCoy's 5A medium, and HK-2 cell lime was cultured in KFSM medium. All media were supplemented with 10% fetal bovine serum (FBS) and 1% penicillin-streptomycin except KFSM medium. All the medium was purchased from Gibco. Cells were cultured at 37 °C in a humidified atmosphere containing 5% carbon dioxide. All cell lines were tested to be free of mycoplasma contamination.

Immunoblotting (ib) And Antibodies

For direct IB analysis, cells were lysed in Radio-Immunoprecipitation Assay (RIPA) buffer with phosphatase inhibitors. The following primary antibodies were used: Cleaved Caspase-3 (Asp175) (5A1E) (#9664), Cleaved Caspase-8 (Asp391) (18C8) (#9496), RB (#9309), p-RB (Ser870/811) (#8516), CDK2 (#2546), p-CDK2 (#2561), Bcl-2 (#15071), Bax (#5023), p21 (#2947), p27 (#3686), Cyclin D1 (#55506), Cyclin E (#4136), p44/42 MAPK (Erk1/2) (137F5) (#4695), Phospho-p44/42 MAPK (Erk1/2) (Thr202/Tyr204) (D13.14.4E) XP (#4370), Akt (pan) (40D4) (#2920), Phospho-Akt (Ser473) (D9E) XP (#4060), PI3 Kinase p110α (C73F8) (#4249), Cyclin A2 (#91500) and Cyclin B1 (#4135) were purchased from Cell Signaling Technology. CDK4 (#11026-1-AP), CDK6 (#14052-1-AP), SKP2 (#15010-1-AP), p53 (1C12) (#2524), P16-INK4A (#10883-1-AP), EGFR (#18986-1-AP) and GAPDH (#60004-1-Ig) were purchased from Proteintech. FLAG was obtained from Sigma-Aldrich (# F1804). As well as all secondary antibodies were purchased from Cell Signaling Technology (Danvers, MA, USA).

Plate Colony-forming Assay

Cells were seeded into six-well plates (Corning, NY, USA) at a density of 500 cells/well. After 24 h, cells were treated with or without nobiletin for 48 h. The nobiletin-containing medium was then removed and replaced by complete medium, followed by incubation at 37 °C for 10-14d. The colonies were fixed with 4% paraformaldehyde, stained with crystal violet, and counted. The colonies composed of fifty or more cells were counted under microscopy. Each experiment was conducted in triplicate.

Lentivirus Or Transient Transfection

For transient transfection, cells were seeded in an antibiotic-free medium at 37 °C for 24 h and transfected with constitutively active SKP2 plasmid or empty vector DNA using Lipofectamine-2000 transfection reagent (Life Technologies, Carlsbad, CA, USA) according to the manufacturer's instructions, and treated 48 h after transfection. The lentiviruses of SKP2 silencing were purchased at Genepharma (shanghai, China), and cells were transfected with lentivirus according to the manufacturer’s protocol.

Apoptosis Analysis

An Annexin V assay was performed according to the manufacturer’s instructions (Life Technologies, Carlsbad, CA, USA). Nobiletin and/or palbociclib treated cells were collected, and used for Annexin V-FITC/PI staining. After that, the samples analyzed via flow cytometry within 1 h. Each experiment was conducted in triplicate.

Cell Cycle Analysis

Cells were collected at the indicated time points after nobiletin and/or palbociclib treated and fixed with ice-cold 70% ethanol, and then stored at 4 °C overnight. After washing twice with phosphate buffered saline, then FxCycle PI/RNAse staining solution (Invitrogen, F10797) was used for detection of cell cycle according to manufacturer’s protocol. These stained cells were subjected to cell cycle analysis using flow cytometer and analyzed for cell cycle phases with C6 Accuri system software. Each experiment was conducted in triplicate.

Cell Viability Assay And Cell Proliferation Assay

The Cell Counting Kit-8 (CCK-8) assay (MCE, HY-K0301) was used to assess cell viability. The cell concentration was adjusted to 2×10^3 cells/well, and the cells were seeded into 96-well plates, followed by 24 h of culture at 37 °C in an atmosphere with 5% carbon dioxide. And then were treated with various concentrations of palbociclib or nobiletin and maintained in culture for 48 h. After removing the culture medium, the CCK-8 reaction solution was added according to the manufacturer’s instructions, and then the absorbance was measured at 450 nm. Half-maximal inhibitory concentration (IC50) value is a critical index of the dose-response curve. Prism statistical software was used to calculate the IC50 values and to plot dose-response curves. According to IC50 values, cells was treated with the given concentration of nobiletin, and cultivation continued for a further 0, 1, 2, 3, and 4d. At different time after cell plating, cells were subjected to the proliferation assay by CCK-8 assay, according to the manufacturer’s instructions. Each experiment was conducted in triplicate.

Cycloheximide Chase Analysis

Cycloheximide chase analysis was performed as described previously to define the effect of nobiletin on the stability of SKP2 protein[29]. Briefly, 786-O and 769-P cell lines (5×10^5) were exposed to 100 μM and 25 μM nobiletin for 24 h, respectively, and followed by 24 h-treatment with cycloheximide (50 μg/mL) (MCE, #HY-12320) to stop de novo protein synthesis. SKP2 levels at 0, 4, 8, 12 and 24 h following cycloheximide co-treatment were then determined by IB analysis. Each experiment was conducted in triplicate.

Quantitative Real-time Pcr

Total RNA was isolated from control and nobiletin-treated cells using RNAisoPlus (Takara, #9108), according to the manufacturer's instructions. Reverse transcription of the extracted RNA to corresponding complementary DNA was performed using PrimeScript RT reagent Kit with gDNA Eraser (Takara Bio, Inc., Otsu, Japan). RT-qPCR was performed with QuantiNova™ SYBR® Green PCR Kit (Qiagen GmbH, Hilden, Germany) on an Applied Biosystems 7900HT Real-Time PCR System. The housekeeping gene, GAPDH, was used as loading controls. The following forward (F) primers, and reverse (R) primers were used: SKP2 forward-CAGGCCTAAGCTAAA TCGAGAG, SKP2 reverse-CTGGCAATGGTGGTGAAATG; GAPDH forward-AG CCTTCTCCATGGTTGGTGAAGAC, GAPDH reverse-CGGAGTCAACGGATTTG GTCGTAT. Each experiment was conducted in triplicate.

Immunohistochemical Staining

Immunohistochemical staining of mice tumors was performed as described previously[30]. Briefly, after deparaffinization, rehydration, antigen retrieval and blocking, the tissue slides were incubated overnight at 4 °C with indicated antibodies. The following primary antibodies were used: Ki-67 (Cell Signaling Technology, #9449), p27 and Cleaved-capase-3.

In Vivo Xenograft Model

Four- to six-week-old BALB/c athymic nude mice (nu/nu, female) were used with each experimental group consisting of five mice. All animal experiments were carried out according to a protocol approved by the University Committee for Use and Care of Animals. 2×10^6 786-O cells were mixed 1:1 with matrigel (BD Biocoat #354230) in a total volume of 200 ul and were injected subcutaneously into right flank side of nude mice. Nude mice were treated with vehicle, nobiletin (40 mg/kg/days, every day, per gavage), palbociclib (120 mg/kg/days, every day, per gavage) or nobiletin + palbociclib when the tumor size reached about 100 mm^3. Nude mice were killed after 21 days of treatment. The growth of tumor was measured twice a week and average tumor volume (TV) was calculated according to the equation: $TV= (L \times W^2)/2$.

Statistical analysis

All data were shown as the average ± standard deviation (Mean ± SD) and each experiment was repeated at least three times independently. All Statistical analyses were performed using the GraphPad Prism Version 5.0 (San Diego, CA). The statistical significance of differences between groups was examined by one-way analysis of variance (ANOVA) followed by Tukey's multiple comparison procedure or student's t test. A *p*-value of less than 0.05 was considered to be statistically significant. Both CalcuSyn software[31] and Jin's formula[32] were used to evaluate the synergistic effects of drug combinations. Jin's formula is given as: Q = Ea + b / (Ea + Eb – Ea × Eb), where Ea + b represents the cell proliferation inhibition rate of the combined drugs, while Ea and Eb represent the rates for each drug respectively. A value of Q = 0.85–1.15 indicates a simple additive effect, while Q > 1.15 indicates synergism. Combination index (CI) plots were generated using CalcuSyn software.

Results

Nobiletin inhibits the proliferation of RCC cells

To identify the inhibitory effect of nobiletin (Fig. 1A) on proliferation of RCC cells, we performed a CCK-8 assay, which revealed that nobiletin significantly inhibited the growth of RCC cell lines in a dose-dependent manner (Fig. 1B). Compared with other RCC cell lines, 769-P cell line had lower response of IC50 of nobiletin (Fig. 1B). Subsequently, we found nobiletin could inhibit the proliferation of 786-O and 769-P cell lines in a time-dependent manner (Figs. 1C&D).

Nobiletin induces G1-phase cell cycle arrest, apoptosis, and colony-forming inhibition in RCC Cells

To clarify the effect of nobiletin in cell cycle arrest and/or apoptosis, we performed flow cytometry and confirmed that nobiletin induced accumulation of G1 phase cell cycle (Fig. 2A and Supplementary Fig. 1A) and elevated apoptotic rates in 786-O and 769-P cell lines (Fig. 2B and Supplementary Fig. 1B), in a dose-dependent manner. Furthermore, nobiletin markedly suppressed the clone-forming ability of 786-O and 769-P cell lines (Fig. 2C and Supplementary Fig. 1C), hence confirming the action of nobiletin to block long-term cell proliferation.

Nobiletin Regulates P21/p27 And Bax/bcl-2

We performed IB analysis to investigate the effect of nobiletin on cell proliferation related signaling pathways. Consistent with G1 phase cell cycle arrest, G1 phase checkpoint protein p21 and p27 were increased by nobiletin (Fig. 3A and Supplementary Fig. 2A). Nobiletin had no effect on CDK2, CDK4 and Cyclin D1 levels, but did dose-dependently reduce expression of p-CDK2, RB and p-RB levels in RCC cell

lines (Fig. 3A and Supplementary Fig. 2A), indicating G1 phase turning to S phase had been arrested. Of course, Cyclin E also was affected by decreasing p-RB (Fig. 3A and Supplementary Fig. 2A). Thus, our findings suggested that nobiletin induced cell cycle arrest in the G1 phase through p21/p27-CKD2-RB pathway, and may thereby prevent tumor progression. Furthermore, levels of Bcl-2 decreased, and levels of Bax increased (Fig. 3B and Supplementary Fig. 2B), suggesting an apoptotic effect of nobiletin on RCC cell lines.

SKP2 downregulation is fundamental for nobiletin induced anti-proliferation in RCC cells

SKP2, well-characterized F-box protein, acts as a classic oncogene which promotes proliferation and survival of cancer cells, mainly through targeted degradation of a number of tumor suppressive proteins, including p21[33], p27[34, 35]. Therefore, we sought whether the increase of p21 and p27 protein levels was related to SKP2 by nobiletin-induced. First, our founding showed that SKP2 levels were markedly decreased in 786-O and 769-P cell lines by nobiletin treatment, in dose-dependent (Fig. 4A) and time-dependent manner (Fig. 4B). We next explored whether nobiletin down-regulated SKP2 by transcriptional and/or post-translational manner. To assess the role of post-translational regulation, 786-O and 769-P cell lines were treated with nobiletin without or with co-treatment of MG-132, followed by SKP2 immunoblotting. Of note, in both tested RCC cell lines, MG-132 co-treatment didn't rescue SKP2 expression to the levels comparable to those of drug-free controls (Fig. 4C). To further substantiated nobiletin-induced SKP2 degradation, we conducted cycloheximide chase analyses, which cycloheximide almost unchanged in the rate of degradation of SKP2 protein in nobiletin-treated RCC cell lines (Fig. 4D). Next, with respect to transcriptional control, we found that SKP2 mRNA levels were noticeably reduced by nobiletin in 786-O and 769-P cell lines (Fig. 4E). Therefore, these results supported that nobiletin-induced SKP2 down-regulation was mainly achieved by targeting SKP2 for transcriptional degradation. Intriguingly, FOXO3 levels were dose-dependently up-regulated in 786-O and 769-P cell lines by nobiletin treated (Fig. 4F). Some papers demonstrated that FOXO3 transcription factor is a negative regulator of SKP2 and SKP2 SCF complex[36]. Based on this, we speculated that the down-regulation of SKP2 might be associated with increasing of FOXO3 levels. Altogether, our results showed that nobiletin regulated SKP2-p21/p27-CDK2 axis to inhibit tumor progression in RCC.

Insensitivity of CDK4/6 inhibitor palbociclib is associated with higher SKP2 levels in RCC cells

CDK4/6-specific inhibitors, such as palbociclib, have shown clinical efficacy, but primary or secondary resistance has emerged as a problem[28]. Our results showed that the doses of palbociclib required to suppress 50% (IC50) of cell proliferation at 48 h were 0.4662 μM, 0.5548 μM, 1.256 μM and 7.718 μM for Caki-1, OSRC-2, 769-P and 786-O cell lines, respectively (Fig. 5A). To confirm the cause of higher concentration of palbociclib to achieve an IC50 response in 786-O and 769-P cell lines, we detected the

expression of related proteins in five renal cell lines, namely Caki-1, 786-O, 769-P, OSRC-2 and HK-2 cell lines. We observed that CDK4, CDK6, CDK2 and p-CDK2 levels were higher (Fig. 5B), as well as lower of p27 levels with higher of SKP2 levels in 786-O and 769-P cell lines (Fig. 5C). p27, as tumor suppressive protein, could influence CDK2[28] and be targeted degradation by SKP2[34, 35], and palbociclib is targeted degradation of CDK4/6. Therefore, we speculated that RCC cells with higher SKP2 levels might require a higher concentration of palbociclib to achieve an IC50 response. We first exogenously overexpressed SKP2 in Caki-1 and OSRC-2 cell lines, followed by treating palbociclib for 48 h. It was showed that SKP2 overexpression of Caki-1and OSRC-2 required higher concentration of palbociclib to achieve an IC50 response than control group (Figs. 6B&C). Simultaneously, as palbociclib high responding RCC cell line, 786-O, was transfected with either control siRNA, or siRNA targeting SKP2 (#228 or #420 or #711), followed by treating palbociclib for 48 h. The dose of palbociclib required to suppress 50% (IC50) of cell proliferation was 7.718 μM for control group, which was least 9 times than SKP2 silencing of 786-O (IC50 (shSKP2-228) = 0.5980 μM, IC50 (shSKP2-420) = 0.6152 μM, IC50 (shSKP2-711) = 0.8326 μM) (Figs. 6D&E&F). From IB results, we found that SKP2 overexpression significantly increased p-CDK2 levels by decreasing p27 levels in Caki-1 and OSRC2 cell lines, and vice versa (Fig. 6A). Thus, we confirmed that insensitivity of CDK4/6 inhibitor palbociclib was associated with higher SKP2 levels in RCC cells.

Dual inhibition of nobiletin and palbociclib shows synergistic lethality in vitro

However, drug toxicity and resistance of palbociclib are still obstacles for its development[28]. Combination with natural compound targeting other pathways may be helpful to reverse drug resistance caused by targeting inhibitors. To determine whether combination of nobiletin with palbociclib have the effects of dual inhibition on RCC cells, we chose the 786-O and 769-P cell lines for the following experiments. Both CalcuSyn software and Jin's formula were used as previously described to determine the synergy of the two agents. 786-O cell line was cultured with combinations of the two drugs at different doses but in a constant ratio (nobiletin to palbociclib: 6.25–0.625 μM, 12.5–1.25 μM, 25–2.5 μM, and 50–5.0 μM, respectively) for 48 h. The combination of 6.25 μM nobiletin with 0.625 μM palbociclib in 786-O cell line inhibited cell proliferation by 32.0%, compared with monotherapy of nobiletin by 15.1% or palbociclib by 11.2%, indicating synergism (CI = 0.905; Q = 0.99; Fig. 7A). Escalating doses, i.e., co-treatment with 12.5 μM nobiletin and 1.25 μM palbociclib (CI = 0.642; Q = 1.10) or 25 μM nobiletin and 2.5 μM palbociclib (CI = 0.585; Q = 1.19) or 50 μM nobiletin and 5.0 μM palbociclib (CI = 0.497; Q = 1.27), showed synergetic effects in 786-O cells (Fig. 7B). Those findings proved that dual inhibition of nobiletin and palbociclib showed synergistic lethality. Furthermore, combination nobiletin with palbociclib strongly induced apoptosis than single agent in 786-O and 769-P cell lines (Figs. 7C&D, Supplementary Figs. 3A&B), which was further demonstrated by the increase of cleavage of caspase-8 and caspase-3 (Fig. 7E and Supplementary Fig. 3C). Similarly, a significant increase of p27 was observed with the combination treatment compared with single agent (Fig. 7E and Supplementary Fig. 3C), suggesting that

simultaneously inhibiting CDK2 and CDK4/6 kinases did more extremely induce apoptosis by combination treatment.

Dual inhibition of nobiletin and palbociclib shows synergistic lethality in vivo

We finally validate the above in vitro findings by using an in vivo xenograft model. A 786-O xenograft model was established and treated with vehicle, nobiletin, and/or palbociclib. Consistent with the in vitro results, the combination of nobiletin and palbociclib suppressed tumor growth significantly more than single-agent treatment (Figs. 8A&B&C). Consistently, the average tumor size and tumor weight at the end of experiment (treatment with 21 days) were significantly lower in nobiletin-palbociclib group (Figs. 8A&C). Body weight of xenograft model was unchanged during drug treatment, suggesting that the effect on normal tissues was minimal (Fig. 8D). Finally, immunohistochemical staining of tumor tissues revealed that compared with nobiletin or palbociclib single-agent treatment, combination of the two agents more significantly inhibited cell growth (decrease of Ki-67 and increase of p27) and induced apoptosis (increase of cleavage caspase-3) (Fig. 8E). Collectively, the combination of nobiletin and palbociclib more significantly inhibited cell growth and survival than single-agent treatment, with less effect on normal tissues. Working model depicting the mechanisms of action underlying nobiletin-induced anti-proliferation. Nobiletin regulated SKP2-p21/p27-CDK2 axis to inhibit tumor progression and showed synergistic chemopreventive effects with palbociclib (Fig. 8F).

Discussion

Polymethoxylated flavonoids (PMFs) have a variety of biological activities such as anti-cancer, anti-cardiovascular disease, prevention and treatment of obesity and anti-inflammatory[37], which are the potential antitumor drugs[7]. Nobiletin is a common PMFs that has been reported to prevent various tumor genesis and development [38, 39]. Several studies have reported antitumor activities of nobiletin, including inhibition of proliferation, cell cycle arrest, and promotion of apoptosis[11, 40, 41]. However, there is still controversy about impact of nobiletin on cell cycle[42] [43]. Meanwhile, there is little evidence to support the use of nobiletin against RCC. Induction of cell cycle blockade underlies one of its anticancer actions but the mechanisms involved are unclear. Therefore, it is important to elucidate the molecular mechanism of nobiletin in cell cycle regulation.

In the present study, we found that nobiletin could inhibit the proliferation of RCC lines in a dose- and time- dependent manners (Fig. 1). Further experiments confirmed that the inhibitory effect was due to the fact that nobiletin could induce G1-S phase arrest in cells (Fig. 2A and Supplementary Fig. 1A). The mechanism was that nobiletin could increase the protein levels of p27 and p21 and then inhibit the activity of CDK2 phosphatase, ultimately leading to the decrease of p-RB (Fig. 3A). p21 and p27 are crucial for restraining the G1-S phase transition[29, 44], and regulated by E3 ubiquitin ligase SKP2 [33–35]. Therefore, we speculated whether nobiletin regulated p27 and p21 by affecting the expression level

of SKP2. Subsequent experiments demonstrated that nobiletin down-regulated SKP2 protein expression in a time- and dose-dependent manners (Figs. 4). In fact, some papers showed that small molecules targeting SKP2 activity or SKP2 complex assembly have been examined in leukemia cells and in xenograft tumor model, respectively, and proved to be effective as anticancer agent[45, 46]. These findings not only provide new insights into the molecular understanding of nobiletin's anti-proliferative effect, but also highlight the potential of nobiletin in the development of SKP2-targeted anticancer therapeutics. It is worth noting that the induction of SKP2 down-regulation and the ensuing p21 and p27 accumulation represented a major mode of action underlying the anti-proliferative effect of a broad range of anticancer agents[29, 47–49]. Next, our finding showed that down-regulation of SKP2 was achieved by inhibiting transcription levels (Figs. 4). Same while, we also find FOXO3 was up-regulated by nobiletin-treated (Fig. 4F). FOXO3 is a transcriptional repressor of SKP2 gene expression by directly binding to the SKP2 promoter [36]. Based on this, down-regulation of SKP2 from transcriptional level is associated with up-regulation of FOXO3 level by nobiletin. Collectively, nobiletin hold great potential for treatment or to serve as a natural and anti-cancer compound by targeting SKP2.

Denovo or acquired resistance to CDK4/6 inhibitors is an almost ubiquitous inevitability. A study has found that palbociclib also inhibited proliferative activity in RCC cell lines, but not all RCC cells were sensitive to palbociclib[26]. We found that 786-O and 769-P cell lines needed high concentration of palbociclib to achieve an IC50 response (Fig. 5A). We observed that CDK4, CDK6, CDK2 and p-CDK2 basal levels were higher (Fig. 5B), as well as lower of p27 levels with higher of SKP2 levels in 786-O and 769-P cell lines (Fig. 5B). As we known, G1/S phase arrest is mainly regulated by two classical cyclin/CDK complex, including cyclinD-CDK4/6 and cyclinE-CDK2[16]. p27 could influence CDK2, and be targeted degradation by SKP2[28, 34, 35]. A study confirmed that while ER positive breast cancer cell lines were inhibited by palbociclib in culture, they quickly adapted because they permitted the degradation of p27 and a subsequent increase in CDK2 activity, allowing compensatory phosphorylation of RB and passage into S phase[28]. Meanwhile, another study also confirmed that CDK4/6 blockade was mediated by the noncanonical CDK2/cyclinD1 complex promoting p-RB phosphorylation recovery. The Cyclin E rebound is likely a consequence of CDK2/cyclinD1 activity and eventually triggering S-phase entry[27]. According to those, we hold that SKP2 was a key target that might provide a therapeutic benefit based on potential resistance of palbociclib. Next, our results showed that palbociclib was more sensitive to silencing of SKP2 group (Figs. 6E&F), and vice versa (Figs. 6B&C). Therefore, sensitivity of palbociclib was associated with SKP2 levels in RCC. High levels of SKP2 are a poor prognostic factor in multiple human cancers[29]. With these notions in mind, searching for agents that reverse resistance of palbociclib represents a promising strategy to discover novel cancer therapeutics[28, 50]. Intriguingly, we investigated that nobiletin could target to down-regulate SKP2 levels to suppressed activation of CDK2 phosphatase (Fig. 3 and Fig. 4). Based on this, 786-O and 769-P cell lines as models to investigate whether nobiletin-palbociclib combination induced apoptosis in RCC cells by dual inhibition. The increase of cleavage of caspase-8 and caspase-3 appeared in combination nobiletin with palbociclib treated RCC cells (Fig. 7E and Supplementary Fig. 3C). Similarly, a significant increase of p27 was observed with the combination treatment compared with palbociclib treatment alone (Fig. 7E and Supplementary Fig. 3C). Similarly, dual

combination of nobiletin and palbociclib significantly inhibited tumor growth in xenograft model (Fig. 8A-E). It is noteworthy that natural compounds could improve the sensitivity and efficacy of chemotherapy drugs[51–53]. To this end, our finding that nobiletin as active component holds great possibilities for reversion of resistance of palbociclib.

To the best of our knowledge, the notion that nobiletin elicits G1 cell-cycle arrest for induction of anti-proliferation (Fig. 8F) through promoting SKP2 degradation has never been reported previously. In conclusion, for the first time, our results demonstrated that nobiletin regulated SKP2-p21/p27-CDK2 axis to inhibit tumor progression and showed synergistic chemopreventive effects with palbociclib in RCC cells. The enhanced anti-cancer effects by the combination treatment were associated with inhibition of cell cycle progression, induction of cellular apoptosis, as well as inhibition of pro-inflammatory cytokines. The fact that combination of nobiletin and palbociclib at their half doses produced stronger anti-cancer effects than nobiletin or palbociclib alone at their full doses provided a strong basis to utilize nobiletin/palbociclib combination for renal cell carcinoma chemoprevention.

Conclusions

In this study, we reported that nobiletin down-regulated SKP2-p21/p27-CDK2 axis to inhibit tumor progression; and nobiletin down-regulated the protein level of SKP2 from the transcriptional level by up-regulating the expression of FOXO3. Meanwhile, Sensitivity of CDK4/6 inhibitor palbociclib was associated with SKP2 levels. Furthermore, dual inhibition of nobiletin and palbociclib showed synergistic lethality in vitro renal cell carcinoma cell model and in vivo nude mice model. To our best knowledge, this is the first study reporting that the mechanism by which nobiletin regulates G1/S block of cell cycle and shows synergistic chemopreventive effects with palbociclib in RCC.

List Of Abbreviations

RCC	Renal cell carcinoma
mRCC	metastatic renal cell carcinoma
OS	Overall survival
PFS	Progression-free survival
CDK2	Cyclin-dependent kinases 2
CDK4/6	Cyclin-dependent kinases 4/6
cDNA	Complementary DNA
DMSO	Dimethyl Sulfoxide
FBS	Fetal bovine serum
RB	Retinoblastoma
GAPDH	Glyceraldehyde-phosphate dehydrogenase
WD/DDLS	Well-differentiated or dedifferentiated liposarcoma
TNBC	Triple negative breast cancer
RIPA	Radio-Immunoprecipitation Assay
SKP2	S-Phase Kinase Associated Protein 2
FOXO3	Forkhead Box O3
PMFs	Polymethoxylated flavonoids
NF-κB	nuclear factor kappa-B
IB	Immunoblotting
qRT-PCR	Quantitative Realtime- polymerase chain reaction
PBS	Phosphate buffered solution
AKT	Threonine kinase
STAT3	Signal transducers and activators of transcription3
CCK8	Cell counting kit-8
IC50	Half-maximal inhibitory concentration
SDS	Sodium Dodecyl Sulfonate
ANOVA	Analysis of Variance
CI	Combination index

Declarations

Availability of data and materials

The datasets used and/or analyzed during the current study are available from the corresponding author on reasonable request.

Acknowledgements

Authors' contributions

L.K.L., W.H.F. and J.X. did the conception and design of the research. T.T.C., L.L. T.Z. and X.Y.H. performed the experiments. T.T.C. interpreted the results of the experiments. T.T.C., L.L. and K.W. prepared the figures. T.T.C. K.W. and X.L. drafted the manuscript. L.K.L., W.H.F. and J.X. edited and revised the manuscript. All authors read and approved the final manuscript.

Funding

This work was supported by the National Natural Science Foundation of China (Grant No. 81772702 to J. Xu; Grant No. 81502214 to WH. Fu).

Author information

Affiliations

Department of Urology, the Second Affiliated Hospital, Third Military Medical University (Army Medical University), Chongqing, P.R. China

Tingting Chen, Xiaoyan Hu & Tao Zhou

Department of Nephrology, Tongji Hospital, Tongji Medical College, Huazhong University of Science and Technology, Hubei, P.R. China

Liu Liu

Department of Hepatobiliary & Pancreatic Surgery, the Second Affiliated hospital of Nanchang University Jiangxi, P.R. China

Kai Wang

Department of Oncology, the First Affiliated Hospital, Third Military Medical University (Army Medical University), Chongqing, P.R. China

Xi Luo

Corresponding author

Correspondence to Longkun Li, Weihua Fu & Jie Xu

Ethics declarations

Consent for publication

Not applicable.

Competing interests

The authors declare that they have no competing interest.

References

1. Siegel, R.L., K.D. Miller, and A. Jemal, *Cancer statistics, 2018.* CA Cancer J Clin, 2018. **68**(1): p. 7-30.
2. Capitanio, U., et al., *Epidemiology of Renal Cell Carcinoma.* Eur Urol, 2019. **75**(1): p. 74-84.
3. Choueiri, T.K. and R.J. Motzer, *Systemic Therapy for Metastatic Renal-Cell Carcinoma.* N Engl J Med, 2017. **376**(4): p. 354-366.
4. Motzer, R.J., et al., *Sunitinib versus interferon alfa in metastatic renal-cell carcinoma.* N Engl J Med, 2007. **356**(2): p. 115-24.
5. Motzer, R.J., et al., *Overall survival and updated results for sunitinib compared with interferon alfa in patients with metastatic renal cell carcinoma.* J Clin Oncol, 2009. **27**(22): p. 3584-90.
6. Beksac, A.T., et al., *Heterogeneity in renal cell carcinoma.* Urol Oncol, 2017. **35**(8): p. 507-515.
7. Mohamed, S.I.A., I. Jantan, and M.A. Haque, *Naturally occurring immunomodulators with antitumor activity: An insight on their mechanisms of action.* Int Immunopharmacol, 2017. **50**: p. 291-304.
8. Park, M.N., et al., *Review of Natural Product-Derived Compounds as Potent Antiglioblastoma Drugs.* Biomed Res Int, 2017. **2017**: p. 8139848.
9. Kumar, A. and V. Jaitak, *Natural products as multidrug resistance modulators in cancer.* Eur J Med Chem, 2019. **176**: p. 268-291.
10. Meiyanto, E., A. Hermawan, and Anindyajati, *Natural products for cancer-targeted therapy: citrus flavonoids as potent chemopreventive agents.* Asian Pac J Cancer Prev, 2012. **13**(2): p. 427-36.
11. Goh, J.X.H., et al., *Nobiletin and Derivatives: Functional Compounds from Citrus Fruit Peel for Colon Cancer Chemoprevention.* Cancers (Basel), 2019. **11**(6).
12. Lien, L.M., et al., *Nobiletin, a Polymethoxylated Flavone, Inhibits Glioma Cell Growth and Migration via Arresting Cell Cycle and Suppressing MAPK and Akt Pathways.* Phytother Res, 2016. **30**(2): p. 214-21.
13. Liu, F., et al., *Nobiletin inhibits hypoxia-induced epithelial-mesenchymal transition in renal cell carcinoma cells.* J Cell Biochem, 2018.
14. Wei, D., et al., *Nobiletin Inhibits Cell Viability via the SRC/AKT/STAT3/YY1AP1 Pathway in Human Renal Carcinoma Cells.* Front Pharmacol, 2019. **10**: p. 690.

15. Stewart, Z.A., M.D. Westfall, and J.A. Pietenpol, *Cell-cycle dysregulation and anticancer therapy.* Trends Pharmacol Sci, 2003. **24**(3): p. 139-45.
16. Asghar, U., et al., *The history and future of targeting cyclin-dependent kinases in cancer therapy.* Nat Rev Drug Discov, 2015. **14**(2): p. 130-46.
17. Fry, D.W., et al., *Specific inhibition of cyclin-dependent kinase 4/6 by PD 0332991 and associated antitumor activity in human tumor xenografts.* Mol Cancer Ther, 2004. **3**(11): p. 1427-38.
18. Reed, A.L., et al., *High frequency of p16 (CDKN2/MTS-1/INK4A) inactivation in head and neck squamous cell carcinoma.* Cancer Res, 1996. **56**(16): p. 3630-3.
19. Lim, J.T., M. Mansukhani, and I.B. Weinstein, *Cyclin-dependent kinase 6 associates with the androgen receptor and enhances its transcriptional activity in prostate cancer cells.* Proc Natl Acad Sci U S A, 2005. **102**(14): p. 5156-61.
20. Young, R.J., et al., *Loss of CDKN2A expression is a frequent event in primary invasive melanoma and correlates with sensitivity to the CDK4/6 inhibitor PD0332991 in melanoma cell lines.* Pigment Cell Melanoma Res, 2014. **27**(4): p. 590-600.
21. Molenaar, J.J., et al., *Cyclin D1 and CDK4 activity contribute to the undifferentiated phenotype in neuroblastoma.* Cancer Res, 2008. **68**(8): p. 2599-609.
22. Kuwahara, Y., et al., *Reexpression of hSNF5 in malignant rhabdoid tumor cell lines causes cell cycle arrest through a p21(CIP1/WAF1)-dependent mechanism.* Cancer Res, 2010. **70**(5): p. 1854-65.
23. Dickson, M.A., et al., *Phase II trial of the CDK4 inhibitor PD0332991 in patients with advanced CDK4-amplified well-differentiated or dedifferentiated liposarcoma.* J Clin Oncol, 2013. **31**(16): p. 2024-8.
24. Dickson, M.A., et al., *Progression-Free Survival Among Patients With Well-Differentiated or Dedifferentiated Liposarcoma Treated With CDK4 Inhibitor Palbociclib: A Phase 2 Clinical Trial.* JAMA Oncol, 2016. **2**(7): p. 937-40.
25. Malorni, L., et al., *Palbociclib as single agent or in combination with the endocrine therapy received before disease progression for estrogen receptor-positive, HER2-negative metastatic breast cancer: TREnd trial.* Ann Oncol, 2018. **29**(8): p. 1748-1754.
26. Logan, J.E., et al., *PD-0332991, a potent and selective inhibitor of cyclin-dependent kinase 4/6, demonstrates inhibition of proliferation in renal cell carcinoma at nanomolar concentrations and molecular markers predict for sensitivity.* Anticancer Res, 2013. **33**(8): p. 2997-3004.
27. Herrera-Abreu, M.T., et al., *Early Adaptation and Acquired Resistance to CDK4/6 Inhibition in Estrogen Receptor-Positive Breast Cancer.* Cancer Res, 2016. **76**(8): p. 2301-13.
28. Patel, P., et al., *Dual Inhibition of CDK4 and CDK2 via Targeting p27 Tyrosine Phosphorylation Induces a Potent and Durable Response in Breast Cancer Cells.* Mol Cancer Res, 2018. **16**(3): p. 361-377.
29. Hsieh, H.Y., et al., *Prodigiosin down-regulates SKP2 to induce p27(KIP1) stabilization and antiproliferation in human lung adenocarcinoma cells.* Br J Pharmacol, 2012. **166**(7): p. 2095-108.
30. Zhou, W.H., et al., *Low expression of Beclin 1, associated with high Bcl-xL, predicts a malignant phenotype and poor prognosis of gastric cancer.* Autophagy, 2012. **8**(3): p. 389-400.

31. TC, C., *Theoretical basis, experimental design, and computerized simulation of synergism and antagonism in drug combination studies.* Pharmacol Rev. , 2006. **58**(3): p. 621-81.
32. Jin, Z.J., *[Addition in drug combination (author's transl)].* Zhongguo Yao Li Xue Bao, 1980. **1**(2): p. 70-6.
33. Yu, Z.K., J.L. Gervais, and H. Zhang, *Human CUL-1 associates with the SKP1/SKP2 complex and regulates p21(CIP1/WAF1) and cyclin D proteins.* Proc Natl Acad Sci U S A, 1998. **95**(19): p. 11324-9.
34. Carrano, A.C., et al., *SKP2 is required for ubiquitin-mediated degradation of the CDK inhibitor p27.* Nat Cell Biol, 1999. **1**(4): p. 193-9.
35. Spruck, C., et al., *A CDK-independent function of mammalian Cks1: targeting of SCF(Skp2) to the CDK inhibitor p27Kip1.* Mol Cell, 2001. **7**(3): p. 639-50.
36. Wu, J., et al., *Foxo3a transcription factor is a negative regulator of Skp2 and Skp2 SCF complex.* Oncogene, 2013. **32**(1): p. 78-85.
37. Manthey, J.A. and N. Guthrie, *Antiproliferative activities of citrus flavonoids against six human cancer cell lines.* J Agric Food Chem, 2002. **50**(21): p. 5837-43.
38. Rodriguez, J., et al., *Effects of several flavonoids on the growth of B16F10 and SK-MEL-1 melanoma cell lines: relationship between structure and activity.* Melanoma Res, 2002. **12**(2): p. 99-107.
39. Kawaii, S., et al., *Effect of citrus flavonoids on HL-60 cell differentiation.* Anticancer Res, 1999. **19**(2A): p. 1261-9.
40. Sp, N., et al., *Nobiletin Inhibits CD36-Dependent Tumor Angiogenesis, Migration, Invasion, and Sphere Formation Through the Cd36/Stat3/Nf-Kappab Signaling Axis.* Nutrients, 2018. **10**(6).
41. Sato, T., et al., *Inhibition of activator protein-1 binding activity and phosphatidylinositol 3-kinase pathway by nobiletin, a polymethoxy flavonoid, results in augmentation of tissue inhibitor of metalloproteinases-1 production and suppression of production of matrix metalloproteinases-1 and -9 in human fibrosarcoma HT-1080 cells.* Cancer Res, 2002. **62**(4): p. 1025-9.
42. Ohnishi, H., et al., *Inhibition of cell proliferation by nobiletin, a dietary phytochemical, associated with apoptosis and characteristic gene expression, but lack of effect on early rat hepatocarcinogenesis in vivo.* Cancer Sci, 2004. **95**(12): p. 936-42.
43. Wu, X., et al., *A metabolite of nobiletin, 4'-demethylnobiletin and atorvastatin synergistically inhibits human colon cancer cell growth by inducing G0/G1 cell cycle arrest and apoptosis.* Food Funct, 2018. **9**(1): p. 87-95.
44. Chu, I.M., L. Hengst, and J.M. Slingerland, *The Cdk inhibitor p27 in human cancer: prognostic potential and relevance to anticancer therapy.* Nat Rev Cancer, 2008. **8**(4): p. 253-67.
45. Chen, Q., et al., *Targeting the p27 E3 ligase SCF(Skp2) results in p27- and Skp2-mediated cell-cycle arrest and activation of autophagy.* Blood, 2008. **111**(9): p. 4690-9.
46. Lin, H.K., et al., *Skp2 targeting suppresses tumorigenesis by Arf-p53-independent cellular senescence.* Nature, 2010. **464**(7287): p. 374-9.

47. Uddin, S., et al., *Bortezomib (Velcade) induces p27Kip1 expression through S-phase kinase protein 2 degradation in colorectal cancer.* Cancer Res, 2008. **68**(9): p. 3379-88.
48. Uddin, S., et al., *Bortezomib-mediated expression of p27Kip1 through S-phase kinase protein 2 degradation in epithelial ovarian cancer.* Lab Invest, 2009. **89**(10): p. 1115-27.
49. Liu, Y., et al., *Imatinib mesylate induces quiescence in gastrointestinal stromal tumor cells through the CDH1-SKP2-p27Kip1 signaling axis.* Cancer Res, 2008. **68**(21): p. 9015-23.
50. Pandey, K., et al., *Molecular mechanisms of resistance to CDK4/6 inhibitors in breast cancer: A review.* Int J Cancer, 2019. **145**(5): p. 1179-1188.
51. Li, S., et al., *Curcumin lowers erlotinib resistance in non-small cell lung carcinoma cells with mutated EGF receptor.* Oncol Res, 2013. **21**(3): p. 137-44.
52. Huang, G., et al., *Aucklandia lappa DC. extract enhances gefitinib efficacy in gefitinib-resistance secondary epidermal growth factor receptor mutations.* J Ethnopharmacol, 2017. **206**: p. 353-362.
53. Song, J., et al., *Combined treatment with Epimedium koreanum Nakai extract and gefitinib overcomes drug resistance caused by T790M mutation in non-small cell lung cancer cells.* Nutr Cancer, 2014. **66**(4): p. 682-9.

Figures

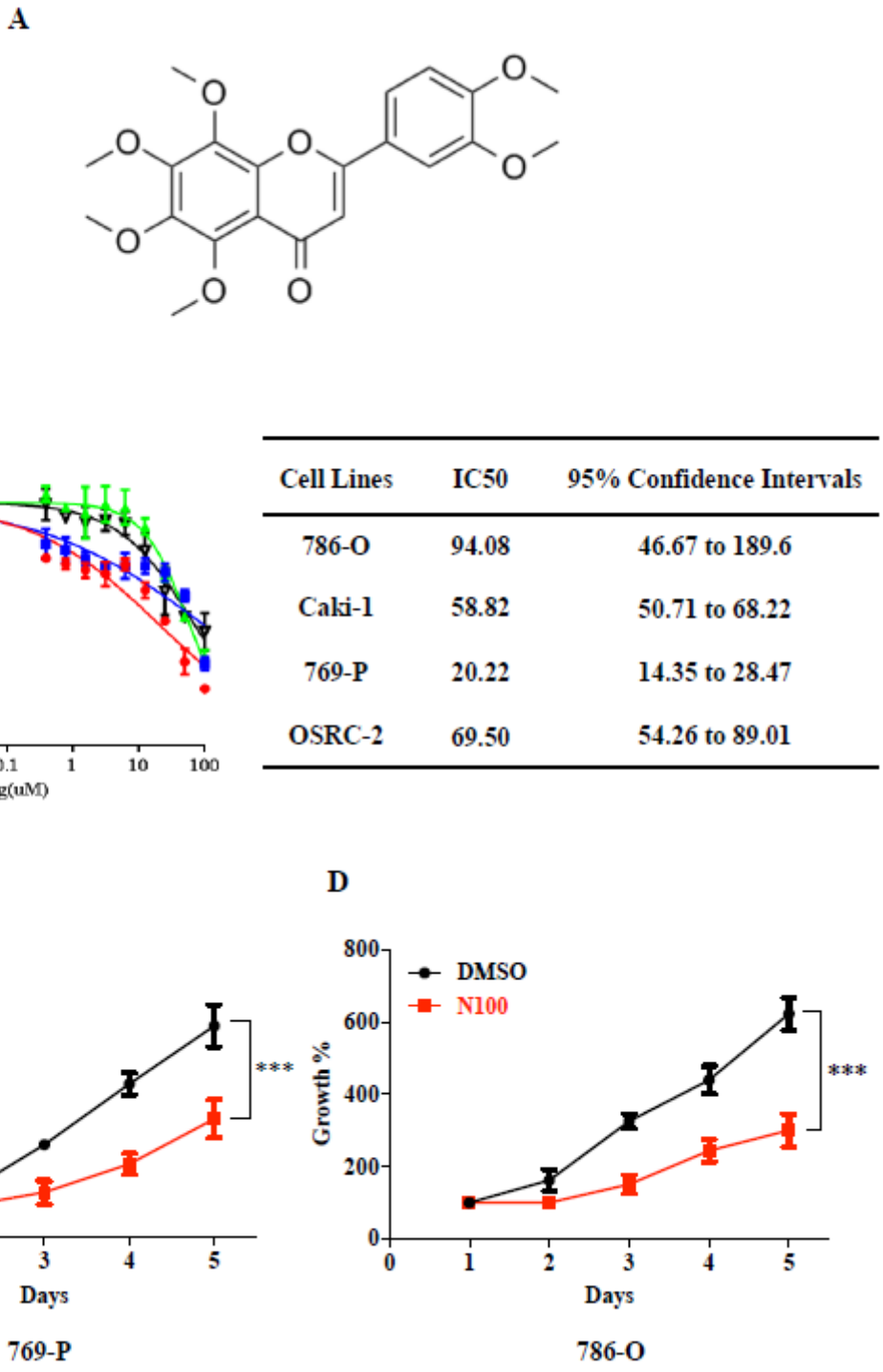

Cell Lines	IC50	95% Confidence Intervals
786-O	94.08	46.67 to 189.6
Caki-1	58.82	50.71 to 68.22
769-P	20.22	14.35 to 28.47
OSRC-2	69.50	54.26 to 89.01

Figure 1

Anti-proliferative action of nobiletin on Renal Cell Carcinoma (RCC) cell lines. A. The structure of nobiletin. B. Dose-response curves of nobiletin against RCC cell lines, after treatment of 48h. Cell viability was detected with Cell Counting Kit-8 (CCK-8) assay. C&D. Nobiletin extremely inhibited RCC cells proliferation in a time-dependent manner. Cultured 769-P and 786-O cell lines were treated in 25μM and 100μM nobiletin for different times, respectively, and then their cellular viability was determined by CCK-8 assay.

Data were presented as means ± SD.*p< 0.05, **p< 0.01, ***p< 0.001, compared with the control group; n=3.

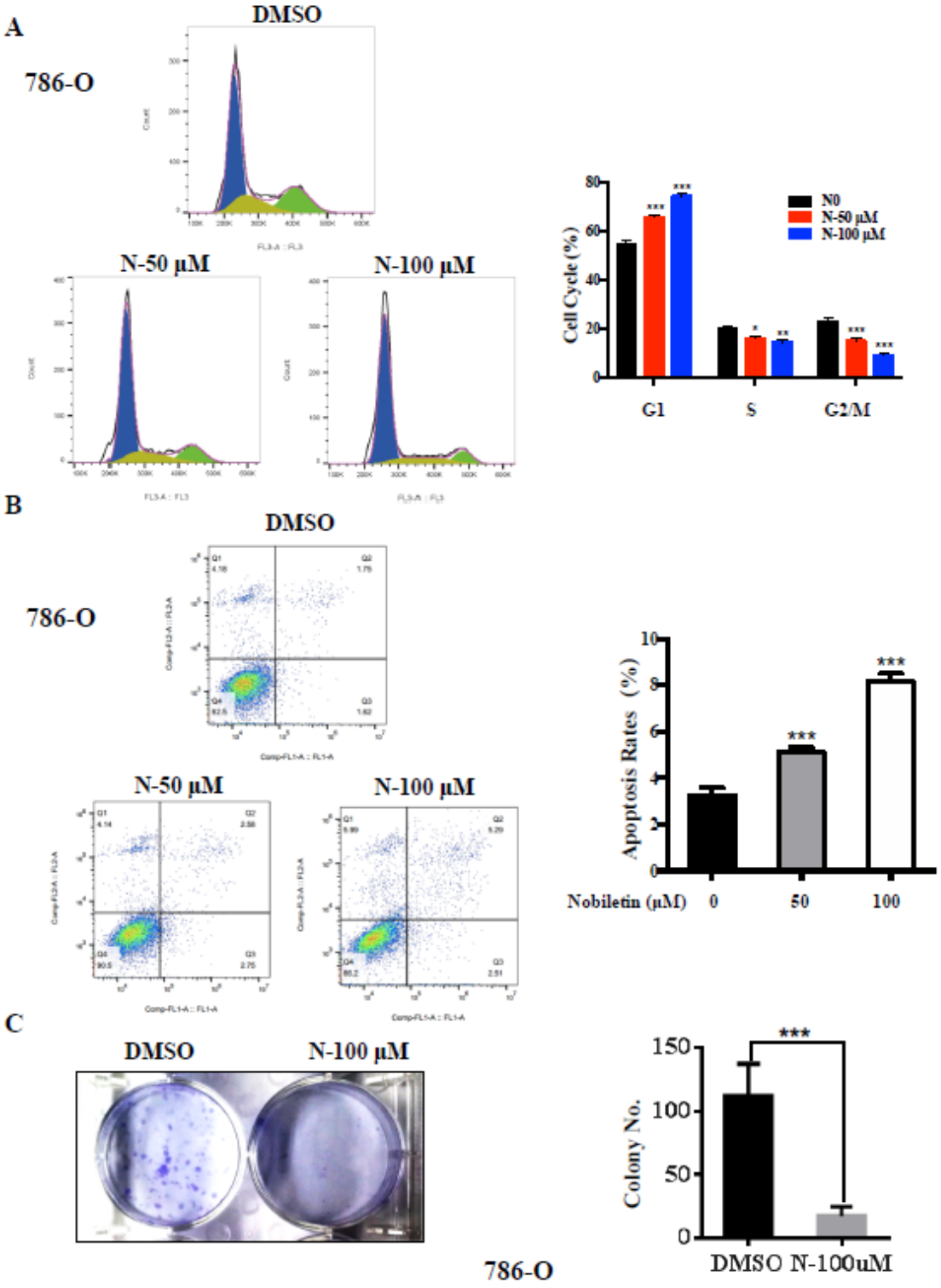

Figure 3

Nobiletin induced G1-phase cell cycle arrest, apoptosis, and colony-forming inhibition in 786-O cell line. A. Nobiletin arrested cell cycle progression at the G1-phase cell cycle in 786-O cell line. 786-O cell line was treated with 50 or 100μM nobiletin for 48h, and cell cycle distributions were then analyzed by flow

cytometry. B. Nobiletin induced apoptosis in 786-O cell line. Apoptosis in 786-O cell line were examined after 48h of treatment with 50 or 100μM nobiletin by annexin V-FITC/PI binding and analyzed by flow cytometry. C. Nobiletin significantly suppressed colony formation in 786-O cell line. 786-O cell line treated with 100μM nobiletin for 48h were allowed to proliferate in drug-free culture media for 10~14d to form colonies, followed by crystal violet staining for scoring colonies. Quantitative results were obtained from the number of colonies. Data were presented as means ± SD. **p< 0.05, **p< 0.01, ***p< 0.001, compared with the control group; n=3.

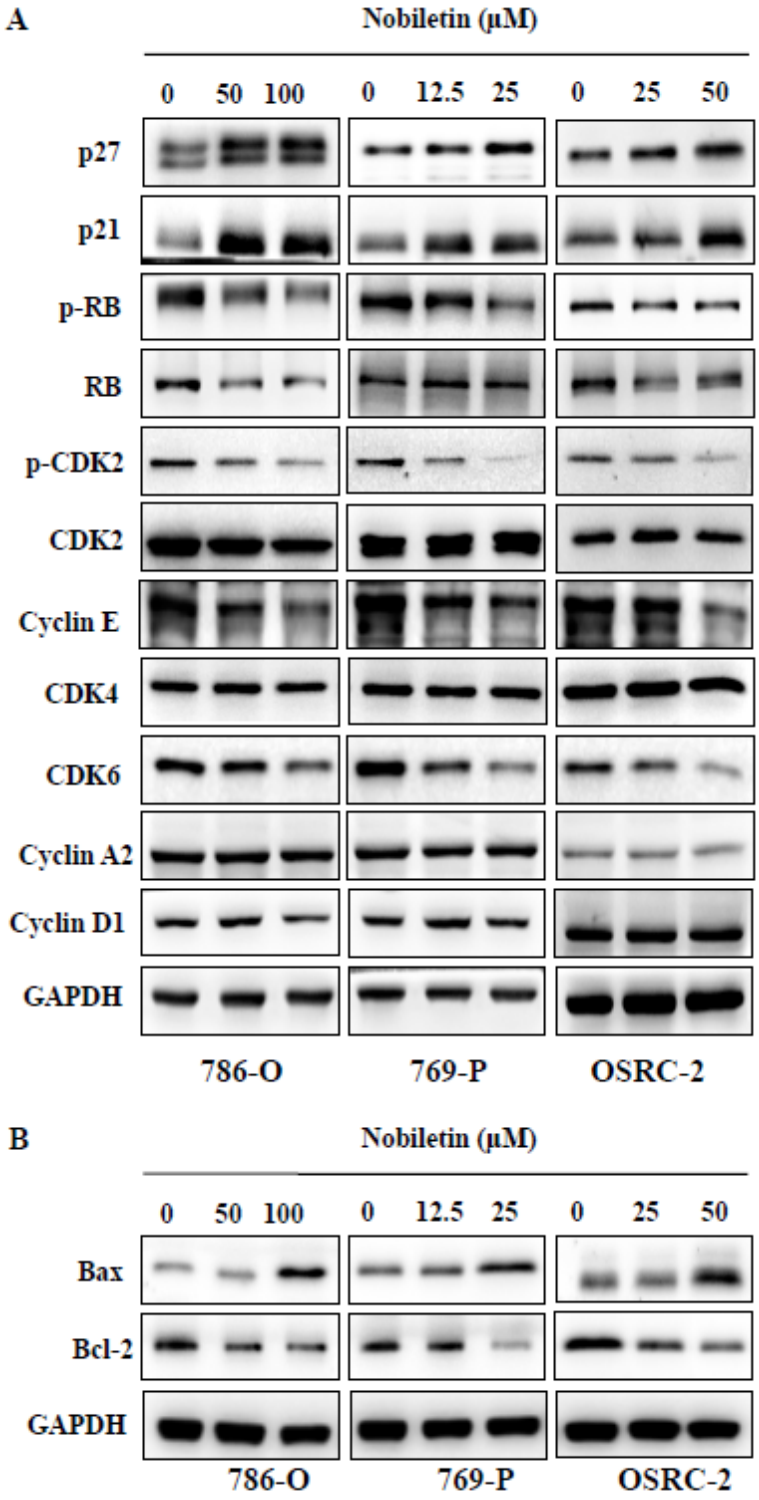

Figure 5

Effects of nobiletin on the expression of cell cycle regulatory protein and apoptosis-related protein in RCC cells. A. Effect of nobiletin on the cell cycle regulatory protein expression in RCC cell lines. RCC cell lines were treated with different doses of nobiletin (50 and 100μM for 786-O cell line; 12.5 and 25μM for 769-P cell line; 25 and 50μM for OSRC-2 cell line) for 48h, followed by determination of related-protein expression using Immunoblotting (IB) analysis. B. Effect of nobiletin on expression of apoptosis-related protein expression in RCC cell lines. RCC cell lines were treated with different doses of nobiletin (50 and 100μM for 786-O cell line; 12.5 and 25μM for 769-P cell line; 25 and 50μM for OSRC-2 cell line) for 48h, followed by determination of related-protein expression using IB analysis. Data were presented as means ± SD. *p< 0.05, **p< 0.01, ***p< 0.001, compared with the control group; n=3. GAPDH levels served as the control for equal loading.

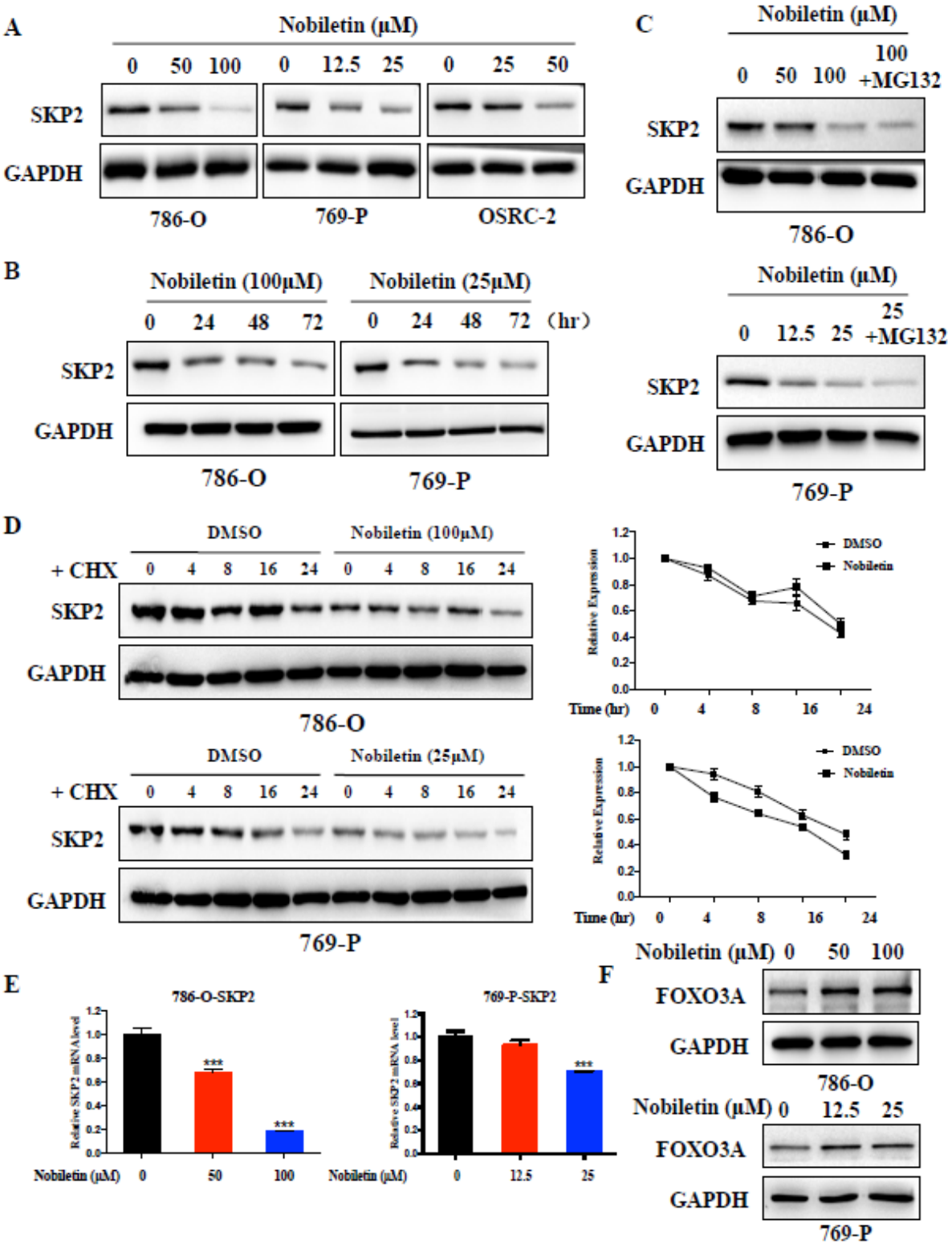

Figure 7

Nobiletin inhibited cell proliferation through down-regulation of SKP2 in RCC cell lines, and SKP2 degradation was mRNA-mediated degradation. A. Nobiletin dose-dependently down-regulated SKP2 levels in RCC cell lines. RCC cell lines were treated with different doses of nobiletin (50 and 100μM for 786-O cell line; 12.5 and 25μM for 769-P cell line; 25 and 50μM for OSRC-2 cell line) for 48h, followed by determination of related-protein expression using IB analysis, followed by SKP2 Immunoblotting. B.

Nobiletin time-dependently down-regulated SKP2 levels in RCC cell lines. Cultured 769-P and 786-O cell lines were treated in 25μM and 100μM nobiletin, respectively, for different times, and followed by SKP2 Immunoblotting. C. Blockade of proteasome-mediated degradation failed to restore SKP2 down-regulation by nobiletin. RCC cell lines were treated with different doses of nobiletin (50 and 100μM for 786-O cell line; 12.5 and 25μM for 769-P cell line) for 24h. The proteasome inhibitor MG-132 was then added to nobiletin-treating cells and the MG-132 co-treatment was allowed to occur for 2h, followed by SKP2 immunoblotting. D. Nobiletin did not destabilize SKP2 levels in RCC cell lines. 786-O and 769-P cell lines were treated with 100μM and 25μM nobiletin for 24h, respectively, and then subject to cycloheximide chase analysis. The levels of SKP2 at 0, 4, 8, 16, and 24h after cycloheximide treatment were determined using IB analysis. E. Nobiletin down-regulated SKP2 levels by regulating SKP2 mRNA level in RCC cell lines. 786-O and 769-P cell lines were treated 100μM and 25μM nobiletin for 48h, respectively, and followed by determination of SKP2 mRNA levels using quantitative real-time reverse transcription-polymerase chain reaction (RT-PCR) analysis. F. FOXO3, as a transcription factor, was up-regulated by nobiletin. RCC cell lines were treated with different doses of nobiletin (50 and 100μM for 786-O cell line; 12.5 and 25μM for 769-P cell line) for 48h, followed by FOXO3 Immunoblotting. Data were presented as means ± SD. *p< 0.05, **p< 0.01, ***p< 0.001, compared with the control group; n=3. GAPDH levels served as the control for equal loading.

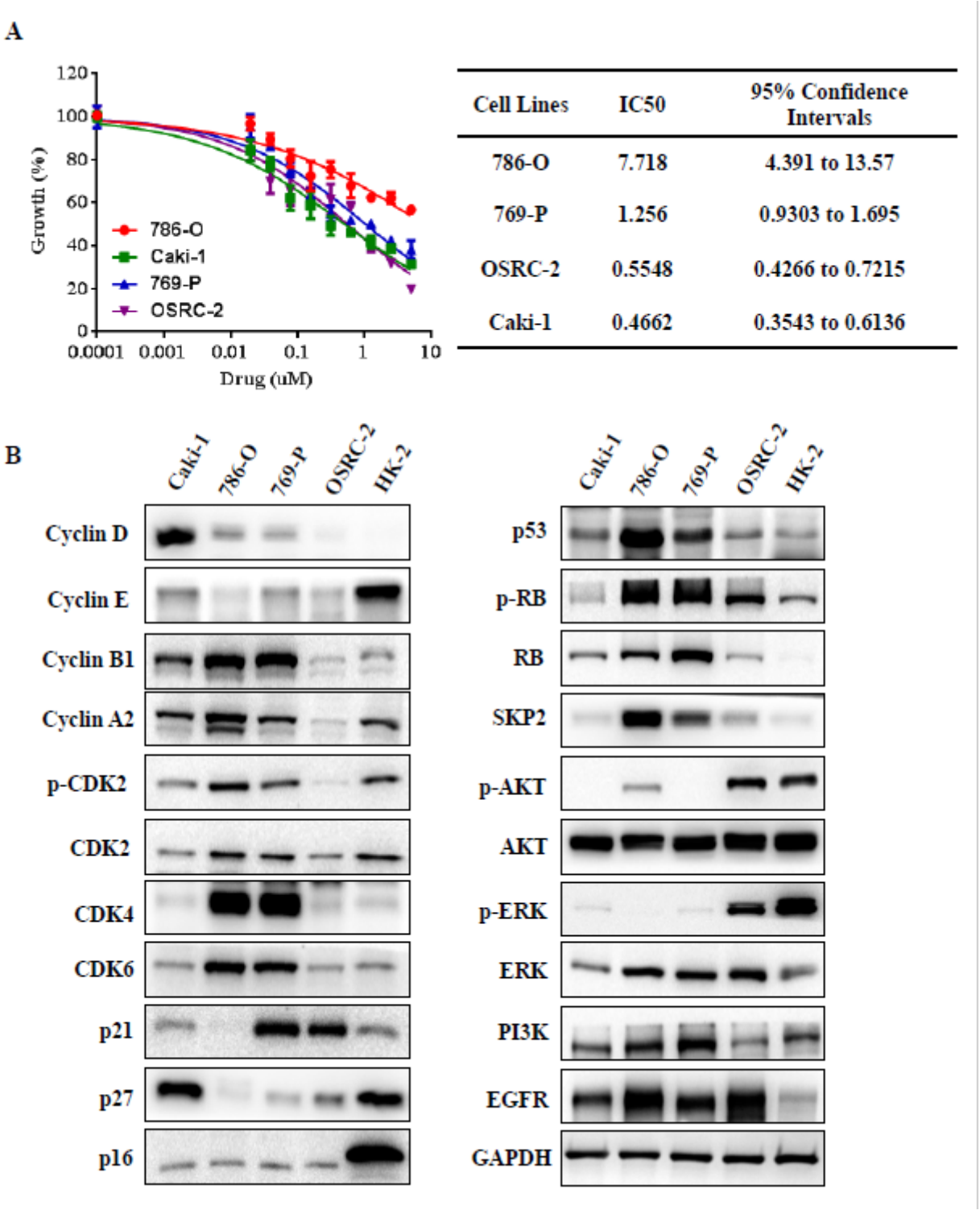

Cell Lines	IC50	95% Confidence Intervals
786-O	7.718	4.391 to 13.57
769-P	1.256	0.9303 to 1.695
OSRC-2	0.5548	0.4266 to 0.7215
Caki-1	0.4662	0.3543 to 0.6136

Figure 9

Anti-proliferative action of palbociclib on RCC cell lines. A. Dose-response curves of palbociclib against RCC cell lines, after treatment of 48h. Cell viability was detected by CCK-8 assay. B. Basal levels of CDK2, CDK4, CDK6, SKP2 and other proteins in RCC cell lines. RCC cell lines were cultured, and followed by determination of protein expression using IB analysis. Data were presented as means ± SD. *p< 0.05, **p< 0.01, ***p< 0.001, compared with the control group; n=3. GAPDH levels served as the control for equal loading.

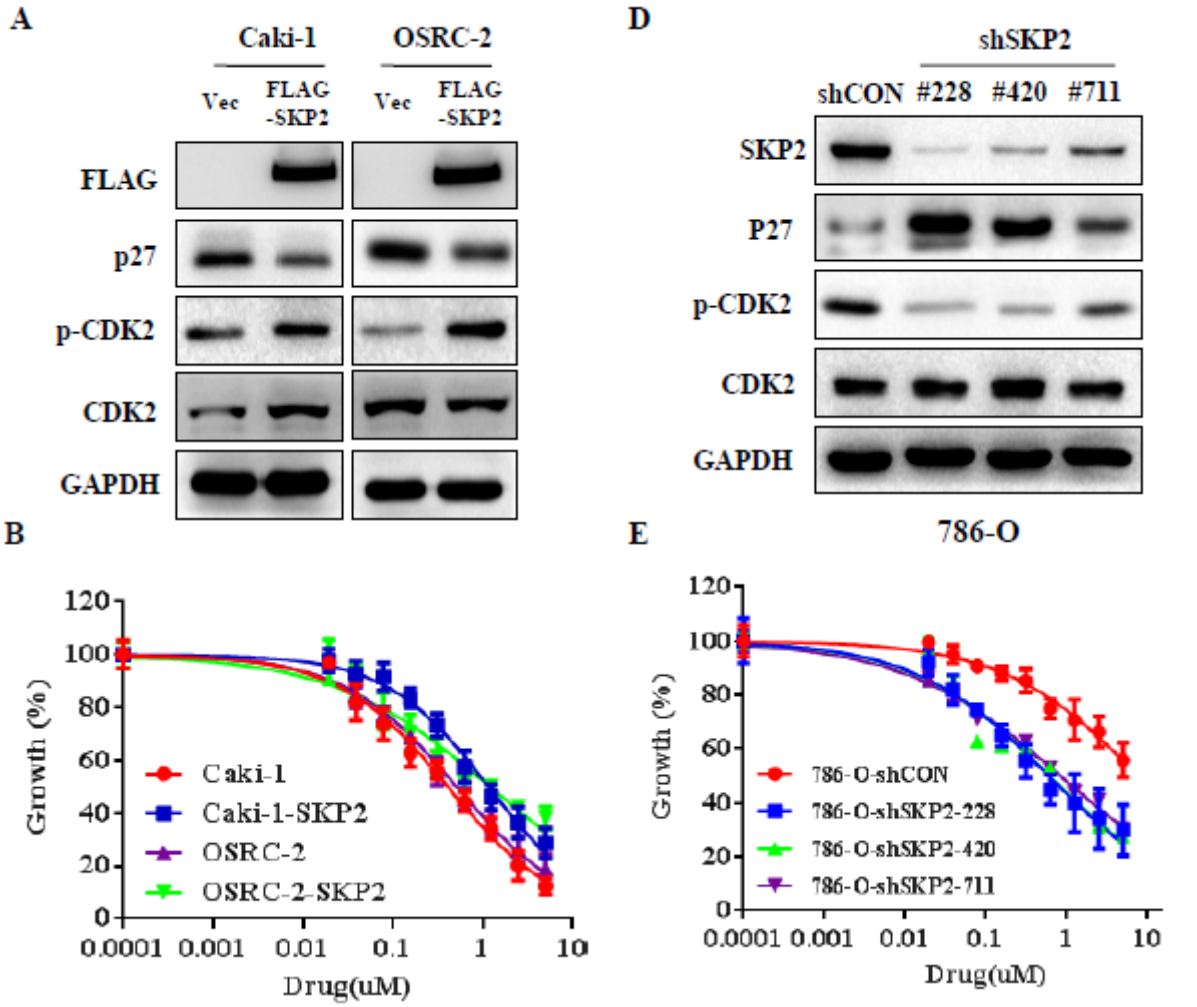

C

Cell Lines	IC50	95% Confidence Intervals
Caki-1	0.4085	0.3510 to 0.4755
Caki-1-SKP2	1.158	1.004 to 1.335
OSRC-2	0.5125	0.4494 to 0.5845
OSRC-2-SKP2	1.199	0.9085 to 1.582

F

Cell Lines	IC50	95% Confidence Intervals
786-O-shCON	7.686	5.346 to 11.03
786-O-shSKP2-228	0.5980	0.4605 to 0.7764
786-O-shSKP2-420	0.6152	0.4853 to 0.7797
786-O-shSKP2-711	0.8326	0.7231 to 0.9587

Figure 11

Sensitivity of palbociclib was associated with SKP2 levels in RCC cells. A. Overexpression of SKP2 attenuated p27 protein levels. p27, p-CDK2 and CDK2 protein expression were determined in stable clones of Caki-1 and OSRC-2 cell lines with ectopic expression of Flag-tagged SKP2. B&C. Overexpression of SKP2 decreased sensitivity of palbociclib-treated RCC cells. Dose-response curves of palbociclib against Flag-taggedSKP2 stable clones and their corresponding vector controls after treatment of 48h. Cell

viability was detected with CCK-8 assay. D. SKP2 silencing increased p27 protein levels. 786-O cell line was transfected with either control siRNA, or shRNA targeting SKP2 (#228, #420, #711), then followed by determination of p27, SKP2, p-CDK2 and CDK2 expression using IB analysis. E&F. SKP2 silencing increased sensitivity of palbociclib-treated RCC cells. 786-O cell line was transfected with either control siRNA, or siRNA targeting SKP2 (#228, #420, #711), and treated with different concentration of palbociclib for 48h. Cell viability was detected with CCK-8 assay. Data were presented as means ± SD. *p< 0.05, **p< 0.01, ***p< 0.001, compared with the control group; n=3. GAPDH levels served as the control for equal loading.

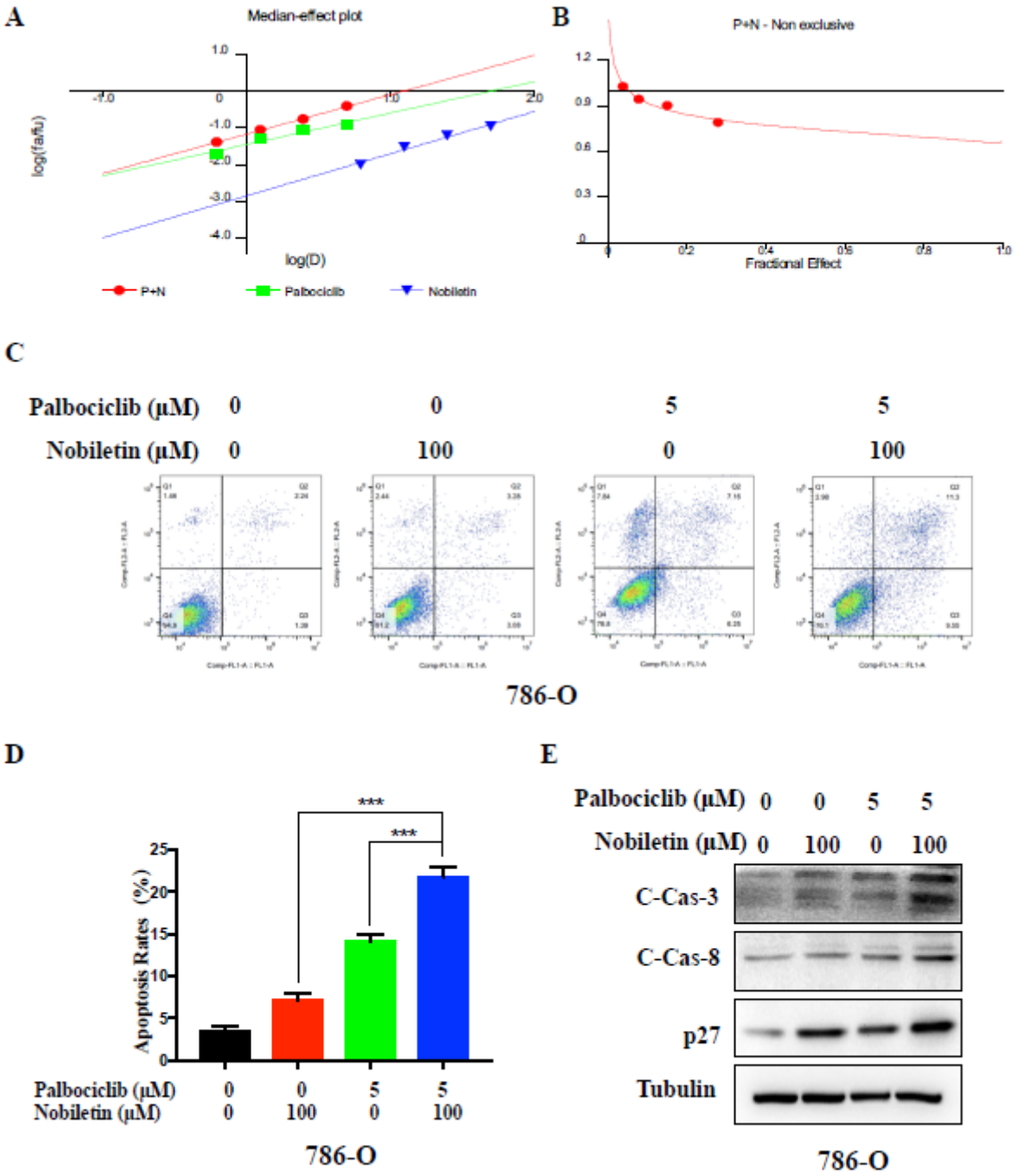

Figure 13

Nobiletin enhanced palbociclib-induced apoptosis in 786-O cell line. A&B. Nobiletin and palbociclib showed synergistic effects in 786-O cell line. CI-effect plots and median effect plots were generated using CalcuSyn software. The points a, b, c and d represent CI values for the combinations 6.25, 12.5, 25 and 50μM nobiletin with 0.625, 1.25, 2.5 and 5μM palbociclb in a constant ratio, respectively. C&D. Nobiletin-palbociclib combination strongly increased apoptosis in 786-O cell line. Apoptosis in 786-O cell line were examined after 48h of treatment with DMSO, 100μM nobiletin, and/or 5μM palbociclib by annexin V-FITC/PI binding and analyzed by flow cytometry. E. Nobiletin-palbociclib combination significantly increased apoptosis-related protein expression in 786-O cell line.786-O cell line was examined after 48h of treatment with DMSO, 100μM nobiletin, and/or 5μM palbociclb, and determined the expression of cleavages of caspase and p27 by IB analysis. Data were presented as means ± SD. *p< 0.05, **p< 0.01, ***p< 0.001, compared with the control group; n=3. GAPDH levels served as the control for equal loading.

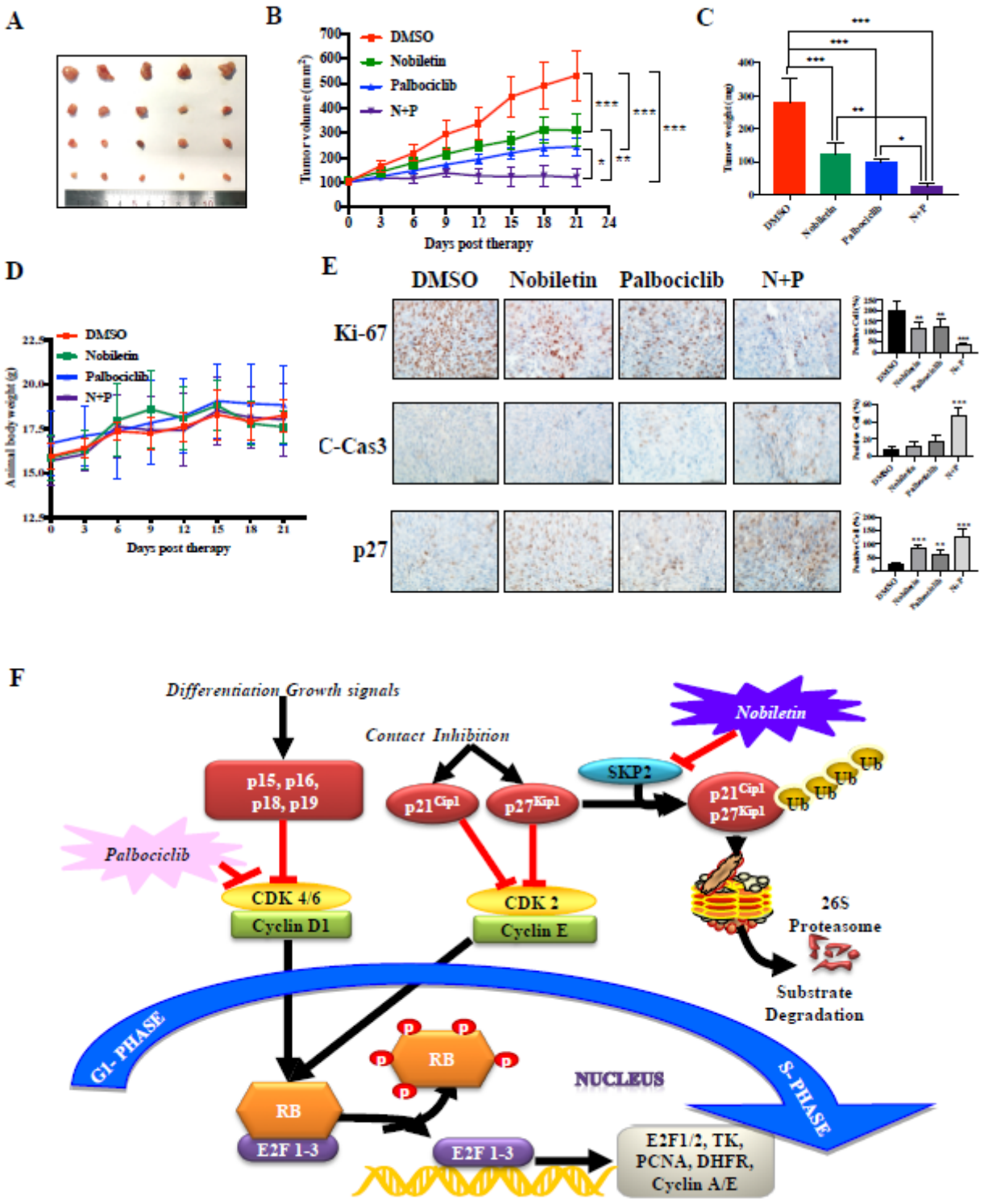

Figure 15

Nobiletin and palbociclib synergistically inhibit RCC tumor growth in xenograft model. A&B&C&D. Synergistic antitumor activity of nobiletin and palbociclib in the 786-O xenograft model. 786-O cell line was injected subcutaneously into right flank side of nude mice. The mice were randomized when the tumor size reached about 100 mm3 and were treated as follows: vehicle, n = 5; nobiletin (40 mg/kg/days for every day for 4 weeks), n = 5; palbociclib (120 mg/kg/days for every day for 4 weeks), n = 5; nobiletin

+ palbociclib, n = 5. The tumor growth was monitored and growth curve was plotted (B) and tumors were harvested and photographed (C) Body weight was measured during the treatment and plotted (D). E. Immunohistochemical staining of xenograft tumor tissues. Tumor tissues from four groups of mice were fixed, sectioned, and stained with indicated antibodies. Scale bars: 100μm. Data were presented as means ± SD. *p < 0.05, **p< 0.01, ***p< 0.001, compared with the control group; n=5. F. Working model depicting the mechanisms of action underlying nobiletin-induced anti-proliferation. Nobiletin targets SKP2 for transcription- mediated degradation to down-regulate SKP2 levels, leading to delayed G1-phase cell cycle progression, and the consequent inhibition of cell proliferation in RCC cell lines. Nobiletin-palbociclib combination induced apoptosis through SKP2-p21/p27-CKD2 -p-RB and cyclinD-CDK4/6-p-RB pathway.

Supplementary Files

This is a list of supplementary files associated with this preprint. Click to download.

- 216Supplementaryinformation.pdf
- SupplementalFigures20200216.pdf
- SupplementalFigures20200216.pdf
- SupplementalFigures20200216.pdf
- 216Supplementaryinformation.pdf
- 216Supplementaryinformation.pdf